Identify Hard-to-Place Kidneys for Early Engagement in Accelerated Placement with a Deep Learning Optimization Approach

Lirim Ashiku¹ and Cihan Dagli¹ Life-Member, IEEE

Abstract— Recommended practices that follow match run sequences for hard-to-place kidneys succumb to many declines, accruing cold ischemic time and exacerbating kidney quality that may lead to unnecessary kidney discard. Hard-to-place deceased donor kidneys accepted and transplanted later in the match-run sequence may threaten higher graft failure rates. Accelerated placement is a practice for Organ Procurement Organizations (OPOs) to allocate high-risk kidneys out of sequence and reach patients at aggressive transplant centers. The current practice of assessing hard-to-place kidneys and engaging in accelerated kidney placements relies heavily on the Kidney Donor Profile Index (KDPI) and the number of declines. Although this practice is reasonable, it also accrues cold ischemic time and increases the risk of kidney discard. We use a deep learning optimization approach to identify kidneys at risk of discard quickly. This approach uses Organ Procurement and Transplantation Network data to model kidney disposition. We filter discards and develop a model to predict transplant and discard of recovered and not transplanted kidneys. Kidneys with a higher probability of discard are deemed hard-to-place kidneys, which require early engagement for accelerated placement. Our approach will aid in identifying hard-to-place kidneys before or after procurement and support OPOs to deviate from the matchrun for accelerated placement. Compared to the KDPI-only prediction of the kidney disposition, our approach demonstrates a ten percent increase in correctly predicting kidneys at risk of discard. Future work will include developing models to identify candidates with an increased benefit of using hard-to-place kidneys.

Index Terms— Accelerated placement, deep learning architectures, hard-to-place kidneys, kidney transplant, optimization.

Affiliations: Missouri University of Science and Technology Systems Engineering, Rolla, Missouri

Corresponding Author: lahnr@umsystem.edu

Abbreviations: AI, artificial intelligence; CIT, cold ischemic time; CNN, convolutional neural network; DEAP, Distributed Evolutionary Algorithms in Python; ID, identification; KDPI, kidney donor profile index; NAS, network architecture search; NM, nautical miles; OPO, Organ Procurement Organization; OPTN, Organ Procurement and Transplantation Network; TXC, transplant center; UNOS, United Network for Organ Sharing.

1 Introduction

Kidney transplantation, including deceased donor kidney transplantation, significantly improves the quality-adjusted life years (QALYs) compared to dialysis [1]. The kidney supply in the United States, the majority of which comes from deceased donors, is limited, fulfilling only 20% of the waitlisted candidate demand [2]. Even with such low supply and high demand, roughly 20% of the recovered deceased donor kidneys are discarded annually [3]. Most of the discarded kidneys have a high Kidney Donor Profile Index (KDPI) which combines ten deceased donor characteristics into a single value to link the possibility of graft failure (immunological rejection) after the kidney is transplanted [3]. Although some kidney discards are unavoidable, it is unclear if an alteration to the current practices of the kidney allocation system could potentially increase the use of high KDPI deceased donor kidneys.

Current kidney allocation practices follow United Network for Organ Sharing (UNOS) policies to match donors fairly and equitably to potential recipients. An organ procurement organization (OPO) is responsible for dealing with all matters related to recovering organs (kidneys), entering all donor medical information into UNOS' network, and allocating organs (kidneys). Similarly, transplant centers (TXCs) enlist transplant candidates and enter medical information into UNOS' network, including dialysis start date, candidate location, medical urgency, etc.

For each donor, OPOs generate a UNOS match-run list to prioritize candidates based on many criteria. Initially, waitlisted candidates found incompatible with the donor will be screened by UNOS; the remaining candidates will be rank-ordered by the UNOS match-run allocation prioritization algorithm that dictates how candidates receive the offers [4]. The OPOs use the UNOS match-run list to present offers to the TXCs listed higher up in the list. Depending upon kidney quality OPOs may increase TXC-batch to offer high-risk kidneys. TXCs have one hour to accept or decline the kidney offer provisionally. The term 'provisionally' implies that for non-primary candidates, the TXC has not made a firm commitment to accept the kidney but rather a tentative interest (candidates not on the top of the match-run list). Provisional acceptances ranked lower in the list become primary when all higher-ranked candidates have declined the offer, in which case an acceptance decision must be made within 30 minutes.

A high-risk deceased donor kidney (KDPI > 80) declined by many TXCs and in a prolonged allocation process (recurrent declines) because of organ quality may be deemed a 'hard-to-place' kidney [5,7]. Declinations of such kidneys may influence the acceptance decision of lower-ranked TXCs, thus increasing cold ischemic time (CIT) for late sequence batch offers and increasing the likelihood of the kidney discard. The effect of increased declinations from higher-ranked candidates and accrued CIT may represent missed opportunities for earlier successful transplants [5] on late sequence batch offers.

UNOS launched a one-year kidney accelerated placement project [6] to increase the utilization of hard-to-place kidneys. Kidneys not allocated within the local or regional area are turned over to the UNOS organ center. UNOS will continue kidney allocation and present the offers to TXCs with prior transplantation of similar kidneys. UNOS accelerated placement project was designed to increase utilization of hard-to-place kidneys (KDPI 80 or higher). However, the UNOS project was only considered for national kidney offers, implying that the kidneys were previously offered to local and regional levels and succumbed to increased declinations and accrued CIT [6]. Figure 1 depicts the highlevel kidney allocation system from the OPO perspective [5-7]. This Figure includes the accelerated kidney placement project for turning over kidney allocation to UNOS. Current practices may be different; depending upon OPO performance, there may be options for OPOs to continue allocation by jumping the list and allocating kidneys using their list of aggressive transplant centers or turning over kidney allocation to UNOS. Similarly, current practices of identifying hard-to-place kidneys may be a combination of characteristics, including KDPI, CIT, and many other logistical variables like proximity, time of the day, etc. [7].

New changes to the kidney allocation system require kidneys to be first offered to the donor hospital's 250-nautical miles (NM) radius [8]. This change prioritizes waitlisted candidates closer to the donor hospital by awarding proximity points reducing travel and minimizing kidney CIT. If offers are not accepted within this radius, then allocation moves outside the circle, and greater proximity points are awarded to candidates closer to the circle. Kidney allocation outside the circle is most likely turned over to UNOS.

According to the Scientific Registry of Transplant Recipients (SRTR), a hard-to-place kidney is a kidney that has previously exceeded 100 TXC offers [9]. Although logistical variables like time of the day, day of the week [10], CIT, etc., may compel accelerated placement, there is no clear-cut representation of when OPOs jump the list for hard-to-place kidneys and engage in accelerated placements. Depending upon the deceased donor's location, US region, or time of the day, logistical variables may have distinct effects on kidney allocation.

Therefore, we propose an AI-enabled approach that can help OPOs deem kidneys hard to place using only donor characteristics. The AI-enabled approach will quickly identify hard-to-place kidneys using broader deceased-donor characteristics instead of the KDPI. The proposed approach has incremental capabilities to predict if a donor's kidney is hard to place before and after procurement. Because there is no distinct feature that shows if deceased donor kidneys were hard-to-

place and presuming that discarded kidneys were hard-to-place kidneys, we consider donor disposition as a target variable. Our proposed method uses a genetic algorithm to optimize and select a deep learning architecture to predict donor disposition, aiding OPOs in identifying hard-to-place kidneys and beginning accelerated placement more quickly. The model is trained using Organ Procurement and Transplantation Network (OPTN) historical deceased-donor data and excludes logistical factors unrelated to deceased-donor kidney quality.

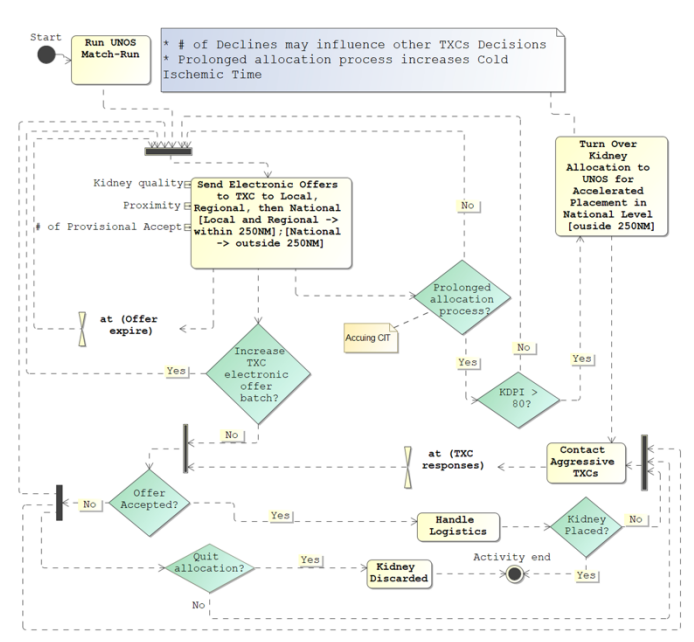


Figure 1. A high-level kidney allocation system from an OPO perspective includes accelerated kidney placement project practices. This Figure represents old policies with different area levels and the new policy with 250 NM. The local and regional are not in perfect correlation with the 250NM policy, but it is included to show at what point kidney allocation is handed to UNOS.

This paper sought to create a model that will aid OPOs in quickly identifying hard-to-place kidneys using donor characteristics. The model uses a deep architecture design and is tuned by a genetic algorithm.

1.1 AI in Healthcare

Machine learning classifiers are used to assess the risk of delayed-graft function in kidney transplants [11]. Among many different classifiers, the authors [11] select random forest and artificial neural networks as the most effective classifiers for the data. Random forest combines the output of many decision trees to a single result, often referred to as an ensemble learning method for classification. An artificial neural network has many (input, hidden, output) layers. Each layer is comprised of neurons connected to preceding and subsequent layers. A deep learning model is used to predict posttransplant renal function in deceased donor kidney recipients using donor biopsy [12]. The authors in [12] conclude that donor kidney biopsy coupled with clinical characteristics to predict graft function improved the prediction accuracy of renal graft function from 0.66 to 0.80.

Similarly, a deep learning model that predicts inpatient acute kidney injury episodes enables the noninvasive kidney disease stage classification using the estimated glomerular filtration rate as a function of patients' serum creatinine [13]. Deep learning or deep neural network uses computational models with layered algorithmic architectures to learn a representation of the input data without explicit guidance from field experts [14]. In addition, deep learning is now being used for coronary artery disease signal identification [15], arrhythmia detection using a different interval of electrocardiogram segments [8], detection of myocardial infarction [16], etc. In liver transplantation, deep learning predicts pretransplant survival in patients with cirrhosis and optimizes donor-recipient fit in the liver allocation system [17].

1.2 Deep Learning Optimization

Despite increasing evidence that deep learning models may outperform expert decision-making and reduce cognitive burden [18], missing data barriers or unbalanced data may cause models to struggle with overfitting. Overfitting is when models closely match training data but do not generalize well on unseen (test) data. Convolutional neural networks (CNNs) are regularized, fully connected networks that overcome overfitting drawbacks [19]. Although CNN models have proven effective, the architecture search is manually designed, requiring users to arrange the width or depth of the architecture initially. In search of optimum architecture, users will perform hyperparameter-tuning and observe if desired performance is achieved. This manual approach has worked well with existing data and is used to develop cutting-edge deep architectures for benchmark datasets [20].

However, users may often find manual hyperparameter-tuning and changes to architecture in search of sub-optimal architecture design are labor-intensive. The search for deep learning network architecture may be partially automated using Grid Search (try hyperparameters from a given set), Random Search (random hyperparameters from a uniform distribution), or a semi-dynamic hyperparameter optimization approach [21]. Automated deep architecture design relies on Neural Architecture Search (NAS) space that grew from Inception [22] to deep architectures with skip connections like ResNet or DenseNet [23].

architecture design has significantly reduced computational resources using parameter sharing in NAS space while achieving similar or better results [20]. Yet, this approach requires an optimization technique deployed in the NAS space to generate high-performing architecture solutions. Common optimization techniques include reinforcement learning, genetic algorithm, and gradient-based descent [20]. Although each has its benefits and drawbacks, the genetic algorithm requires greater preparation to establish search space and develop network representation but improves architecture solutions. The genetic algorithm that allows parameter sharing across generations enables rapid training (inherited weights) of matching architectures. The approach discussed by [20] built upon blocks comprised of various layers and represented as chromosomes, and each value in the chromosome denotes an operation for the layer. However, the deficiency of hyperparameter tuning makes the latter approach appropriate for deep neural architecture search when scarce computational

On the other hand, DeepMaker is used to develop network optimization by (1) design space exploration that searches for

design configurations, including hyperparameter tuning and architecture design, and (2) minimizing computation power required by removing redundant filters known as network pruning [24]. To minimize computational resource utilization, DeepMaker searches for sub-optimal network architectures by partial training deeming 16 epochs sufficient for achieving 90% accuracy. The multi-objective optimization strategy of design space and network pruning provides a framework for attaining sub-optimal models at much reduced computational resources. However, the multi-objective tradeoff of DeepMaker leaves other areas for exploring, including the geometric dimensions of each layer. Training deeper networks doesn't necessarily mean better performance than shallow ones, but deeper networks can represent compositionality and adapt to prior information [25]. Conversely, deep networks suffer from degradation problems like overfitting, vanishing gradients, or exploding gradients. Skip connections such as ResNet, DenseNet, or GoogLeNet are introduced to handle deep network degradation problems, which use identity mapping to bypass residual layers and preserve low-level features [26,27].

2. METHODOLOGY

2.1. Data Preprocessing

This study used OPTN deceased donor data to train and test a hard-to-place kidney model. The OPTN data repository includes data on donors, waitlisted candidates, and transplant recipients. The transplant recipient data is usually linked with match runs and is provided with an ID to link with waitlisted candidates. All data, apart from match runs and images (if available), can be available upon request.

However, the data has many missing values for older observations; therefore, we considered the most recent UNOS deceased-donor data from January 1, 2015, to June 30, 2021. @ Furthermore, we isolated and compared distinct right and left kidney characteristics and found significant differences in procurement biopsies. Therefore, we created two copies of the data that isolated characteristics belonging to either right or left kidney. The isolations were caused by the aggregate kidney disposition label *KIB DISPOSITION that didn't reflect the sum of its parts (right *KIR DISPOSITION and left *KIL DISPOSITION kidney disposition). Additionally, for the target variable of the kidney disposition label, we only used data observations for recovered deceased donor kidneys that were either transplanted or not transplanted. To identify whether the 'not transplanted' kidneys were discarded, we conducted a comparative analysis using the number of kidneys recovered *NUM KI RECOV, kidneys transplanted *NUM KI TX, and kidneys discarded *NUM KI DISC. Observations for kidneys not recovered, or not recovered for transplant, and authorizations not requested or obtained are dropped from the data.

Table 1 shows the principal components contributing to the target variable's total variance in impact score obtained by principal component analysis. The principal component analysis uses statistical analysis to extract meaningful information from large datasets and summarize it with a smaller set of components. The new donor characteristics/components are ordered by impact score (total variance explained by the component). Pearson's correlation measures the linear correlation between two components; the negative value

denotes an inverse relationship between the target and the component.

On the other hand, KDPI will be used as ground truth and, therefore, not included in the model but instead regressed from the features presented. Other redundant features, such as body mass index, hypertension duration, expanded criteria donor, etc., have a greater impact score than the correlated features. Since they can be inferred from the remaining features, we excluded them from the data.

 $\label{thm:table1} TABLE\ 1$ PRINCIPAL COMPONENTS, IMPACT SCORE, AND PEARSON'S CORRELATION

Component	Impact Score	Pearson's Correlation
Kidney Glomerulosclerosis	11490	-0.478
Donor Age	8529	-0.365
History of Hypertension	5385	-0.297
Glomeruli Count	3795	-0.237
Serum Creatinine	3611	-0.212
Coronary Artery Disease	1933	-0.184
Blood Urea Nitrogen	1618	-0.168
History of Cancer	1090	-0.084
History of Diabetes	798	-0.057
Donor Weight	682	-0.054
Donor Height	632	0.052
Donor's HCV Status	598	-0.077
Donor meets DCD Criteria	487	-0.064
History of Cigarette Use	443	-0.141
RNA Nat serology HBV-	421	-0.094
Test		
Arginine	405	0.085
Cause of Death	327	-0.004
Donor pH Level	317	0.102
Donor Gender	312	0.061
Kidney on Pump	161	0.048
Clinical Infection	104	0.042
Ethnic Category	72	0.022
Clamp Time	31	-0.007
KDPĪ	(Not used in the model)	
Cold Ischemic Time	(Not used in the model)	

Because we were predisposed to KPDI-driven characteristics, we also included the ethnic category, which ranks lower than clinical infection, donor smoking history, donor pH level, etc. Table 2 displays the principal components of the deceased donor data used to train the model. Table 2 includes the nature of the data population and the percentage of the categorical observations.

Since features like pump device, initial flush solution, final flush solution, and biopsy type are not among the principal components, we ignored them. Similarly, all features linked with the aggregate kidney effect (both kidney labels) were deemed ineffective because the target didn't reflect the sum of its parts and dropped from the final data used to train the model.

 ${\bf TABLE~2}$ Principal characteristics of the deceased donor population

Parameter	Population (Mean \pm Standard Deviation) Categorical shown by % of observations Number of observations (N = 63,295)
Donor Age (years)	40.51 ± 15.72
Ethnic Category	67.24% White, 14.38% Black, 14.07% Hispanic, 2.50% Asian, 0.90% Multi-Racial, 0.61% Am-Indian, 0.29% Pacific

Donor Height (cm)	170.25 ± 13.40
Donor Weight (kg)	82.99 ± 23.67
Donor meets DCD Criteria	77.35% No, 22.65% Yes
Donor Gender	61.09% Male, 38.91% Female
History of Diabetes	88.67% No, 4.13% 0-5yrs, 3.03% >10yrs, 2.02% 6-10yrs, 1.23% Duration-Unknown, 0.91% Unknown
History of Hypertension	67.25% No, 14.07% 0-5yrs, 7.87% >10yrs, 6.29% 6-10yrs, 4.51% Unknown
Serum Creatinine	1.41 ± 1.34
Cause of Death	42.70% Anoxia, 28.16% Head trauma, 26.02% Cerebrovascular, 2.77% Other, 0.33% CNS tumor
Donor's HCV status	92.97% Neg, 5.21% Pos, 1.69% Not done, 0.009% Inconclusive, 0.001% Unknown
Coronary Artery Disease	92.98% No, 5.64% Yes, 1.37% Unknown
History of Cancer	96.13% No, 2.96% Yes, 0.91% Unknown
Kidney on pump	60.61% No, 38.17% Yes, 1.14% Unknown
Kidney	44.70% NA, 34.52% 0-5, 8.51% 6-10,
Glomerulosclerosis	5.35% 20+, 4.18% 11-15, 2.45% 16-20, 0.27% Unknown
Kidney Glomeruli count	32.22 ± 39.76
Blood Urea Nitrogen	24.52 ± 19.17
History of Cigarette Use	76.69% No, 21.20% Yes, 2.11% Unknown
RNA Nat ser- HBV Test	95.14 % Neg, 4.74% Pos, 0.11% Not done
Arginine	48.97% Yes, 39.30% No, 11.73% Unknown
Donor pH Level	7.40 ± 0.08
Clinical Infection	73.68% Yes, 24.34% No, 1.98% Unknown
Clamp Time	12:55 PM \pm 7
KDPI	47 ± 29 (not used in the model)

Since roughly 20% of the kidneys are discarded [2,3], we have a 4:1 class imbalance. We sampled the data using the synthetic minority oversampling technique (SMOTE) and class weight to address the class imbalance. SMOTE is applied only to the training data, and the class weight corresponds to a weight based on the number of observations per class.

2.2 Model Development Approach

Model development with shallow networks such as decision trees, regularized regression, random trees, and shallow artificial neural networks was attempted and generated promising results compared to the KDPI ground truth [28]. However, the shallow network hyperparameter tuning is limited, and so are model performance improvements. Therefore, we use a deep optimization approach that presents an automated, efficient deep architecture search incorporating hyperparameter tuning and geometric dimensions that handle degradation problems [20,25,26]. CNNs as regularized artificial neural networks have penetrated a broad spectrum of leveraging high-performance architectures classification and computer vision. We use a single objective evolutionary genetic algorithm to search the NAS space and rank populations (a subset of deep learning architecture) as fitness functions (accuracy in predicting hard-to-place kidneys). A genetic algorithm is a subclass of evolutionary algorithms motivated by a human genetic process used for optimization and search space problems [29]. Initially, a random population (set of solutions) is generated. The population is represented using binary bits outlining a set of properties (chromosomes).

These chromosomes outline the hyperparameters of the deep network architecture. Crossover and mutation are used to diversify the population. Crossover is applied to two chromosomes to generate a second-generation population. Crossover can be applied at a single-point, two-point, or k-point, where k is any positive integer less than the number of genes in the chromosome. In a single-point crossover, the leading part of the first chromosome is joined with the trailing part of the other. The k-point crossovers follow the same pattern as a single-point but repeated k-times.

Similarly, mutation generates new chromosome properties by bit flips at a random position of the chromosome [30]. The reproduction process depends on the fitness of the latest population in predicting kidney disposition. Chromosomes with better fitness replace current individuals in the hall of fame 'elitism' and are used for breeding the next generation. Table 3 depicts the step-by-step process of the genetic algorithm deep architecture search.

TABLE 3
GENETIC ALGORITHM DEEP ARCHITECTURE SEARCH

Algorithm: The genetic algorithm for deep architecture search

- 1. Input: OPTN data, the number of generations G, and the number of individuals for each generation N
- **2. Initialization:** generate a set of randomized chromosomes to represent all properties of the deep network architecture defined as the initial population.
- **3. Evaluation:** compute the fitness function of chromosomes in the population
- **4. Iteration:** repeat the process until the stop criterion is satisfied or time t=G
- **5. Crossover:** a single-point crossover using two chromosomes.
- 6. Mutation: a flip-bit mutation on new chromosomes.
- **7. Evaluation:** compute the fitness function of chromosomes in the population
- **8. Elitism:** current x-best (hall of fame) individuals/chromosomes are passed to the next generation
- 9. Repeat from step 4
- 10. Output: display the average of the 'hall of fame' individuals and the best solution.

The evaluation computes the fitness function of the chromosomes in the population. We used Distributed Evolutionary Algorithms in Python (DEAP) for optimizing deep architecture [31]. DEAP is an evolutionary computation framework providing the essentials for users to customize functions and fit the current optimization problem [32]. The DEAP 'toolbox' is a wrapper container leveraging functionality in creating individuals, crossover, mutation, etc., but requires adequate user knowledge to deploy.

Table 4 depicts the genes within the chromosome, their explored ranges, and the number of bits within the chromosome representation. Since artificial neural networks are seen as mathematical models designed to recognize patterns and learn like the human brain, we attempt to describe hyperparameters with an analogy to the human brain. The optimization block (Oblock), like the nervous system, is the property used to configure the number of systems needed to generate a best-fitted population. The internal components of O-blocks do not change from one block to another. The activation functions, like synapses, are used to introduce nonlinearity into the output of a neuron. The convolutional layers, like the number of

synchronous groups of connections, are used to aid in capturing features that may otherwise be missed during processing. The convolutional layer is CNN's fundamental building block that comprises most computations. The learning rate is like the neuronal processing speed. Kernel size is used as a filter to extract (sample) features analogous to the receptive field of the retinal ganglion [33]. Cost functions calculate the error between the predictions and the actual outcome during the training phase. Dropouts are skipped connections to prevent memorization and overfitting. Hidden layer neurons represent the number of neurons within a convolutional layer. Geometric dimensions like dendritic patterns are provided as properties in search of the best chromosomes [34].

Table 4 depicts the hyperparameters for the deep architecture NAS space. The suggested values are not all-inclusive but are common parameter values across the deep learning realm. Each hyperparameter/property can be represented in binary using 1, 2, or 3 genes/bits. This Table is for information only; we will illustrate a full scale of deep learning optimization on the paper in preparation (L. Ashiku, C. Dagli, unpublished data, October 2022). Deep aggregation is used to help recover spatial information or boundary localization while merging O-blocks [35].

TABLE 4
CNN HYPERPARAMETER TUNING OPTIONS

Parameters	Values	Genes/Bits
Optimization	1, 2, 3, 4,8	3 bits
block		
Activation	Linear, Sigmoid, Tanh, ReLU,	3 bits
function	LeakyReLU, Hard-sigmoid, Swish, Softplus	
Convolution layers	4 6 8 10	2 bits
Learning rate	$10^{-3} 10^{-4} 10^{-5} 10^{-6}$	2 bits
Kernel size	3x3 5x5	1 bit
Cost function	SGD, SGD-M, AdaGrad, RMS-Prop, AdaDelta, Adam, Adamax, Nadam	3 bits
Dropout	.2 .3 .4 .5	2 bits
Hidden layer neurons	16 24 32 64	2 bits
Geometric	VGGNet, ResNet, DenseNet,	2 bits
dimension	GoogLeNet	
Deep aggregation	0 1	1 bit

Parameter values choices are represented by a factor of two to aid GA chromosome bit-representation.

Figure 2 illustrates a generic deep architecture comprised of back-to-back O-blocks for feature extractions that includes many convolutional layers. Each convolution layer has batch normalization, activation function, learning rate, kernel size, hidden layer neuron, and dropout regularization. Geometric dimensions connect the convolutional layers. Deep aggregation is external to O-block and joins final convolution layers of O-blocks to deepen the architecture while progressively refining the representation. Finally, the cost function is used to evaluate a candidate solution in terms of prediction to actual output error.

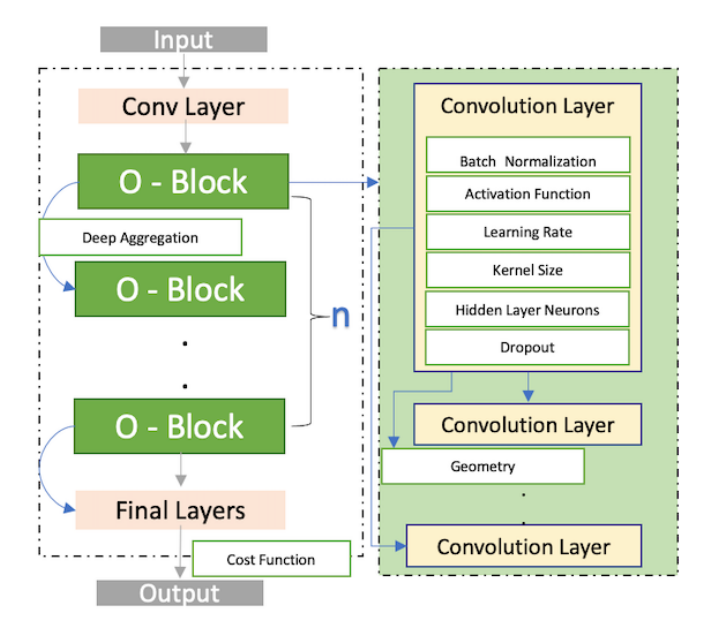


Figure 2. O-block hyperparameters represent the deep architecture. On the left, we depict the O-blocks as intermediate between the input and output layers (n). The genetic algorithms select the number of convolutional layers. Each convolutional layer contains all hyperparameters shown within the layer. Geometry represents the convolutional layer patterns within an O-block.

Figure 3 illustrates the genetic algorithm process to induce diversity in the population. The chromosome is represented in 21 bits; the first 3 bits represent O-block size. The next 3 bits represent the activation function within the convolution layer, followed by a 2-bit representation of the learning rate. The kernel layer is shown with a single bit, followed by a 3-bit cost function representation. Dropout regularization, hidden layer neurons, and geometric dimension are each represented by 2 bits. Finally, deep aggregation is shown using a single bit. Two selected chromosomes from the random population are chosen to induce the new individuals [38]. A single-point crossover generates two new chromosomes using genes of the previous generation. Finally, gene mutations produce new chromosomes that will be evaluated on the accuracy of predicting kidney disposition to identify hard-to-place kidneys.

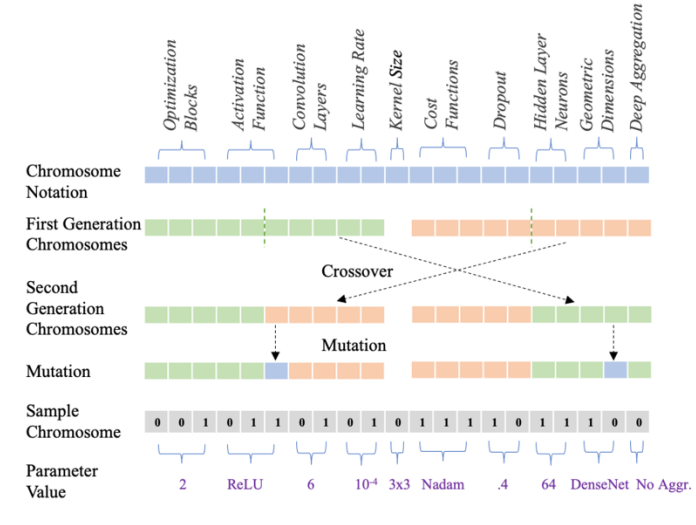


Figure 3. Chromosome notation and the application of a genetic algorithm to induce a new population. Each segment of the chromosome is shown in terms of the hyperparameters. Two first-generation chromosomes are used to create a

second-generation chromosome after crossover. The second-generation chromosome is then mutated, and a new population is created. The sample chromosome is illustrated by the parameter values shown in Table 4.

3 RESULTS

The two copies of the data that isolated characteristics of either right or left kidney for the kidney disposition model produced results that were not statistically different; therefore, the results reflect only the right kidney disposition. To set the stage for ground truth, we revisit common practices for early engagement in accelerated placement. The current practice of assessing hardto-place kidneys and engaging in accelerated kidney placement may vary from one OPO to another. Some OPOs may associate with SRTR definition for hard-to-place when deceased donor kidneys exceed 100 declinations and have KDPI > 85 [9]. Other OPOs may constitute other internal policies and accelerate placement when kidney allocation within 250NM is unsuccessful, serum creatinine is increased, and CIT accrued 6 hours. Similarly, procurement biopsy results may deem kidneys hard to place and increase the discard rate for kidneys with lower KDPI scores [36]. Since the proposed model can be used to assess kidney disposition before and after procurement, we will create three baseline models: 1. using only KDPI, 2. using KDPI and serum creatinine, and 3. using KDPI, age, and procurement biopsies [37,38]. The proposed model will be an incremental model using OPO-current data to assess kidney disposition before and after procurement. The model excludes CIT (not available for discarded kidneys) and the number of offer declines (not incorporated in the deceased donor dataset due to high variability in OPO practices of accelerated placement and offer bypass coding). Figure 4 illustrates the kidney disposition results obtained from the genetic algorithm deep architecture search compared to the baseline (KDPI-only). The best architecture represents the individual with the highest fitness function on a full-scaled after-procurement model, excluding KDPI from features represented in Table 2. The KDPI-only model represents the best deep learning architecture for a single input feature. The average model represents the elite population replaced only by better individuals. Finally, the KDPI-characteristics model represents the deep learning architecture to predict kidney disposition using the ten characteristics that regress KDPI.

Kidney disposition prediction for selected architectures

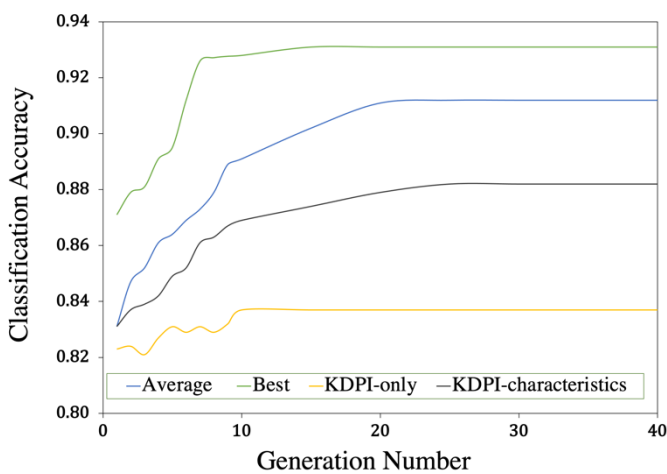


Figure 4. Kidney disposition prediction fitness (accuracy) for the optimized deep learning architectures. The genetic algorithm is optimized only for the full-scale after-procurement model that uses clinical donor characteristics shown in Table 2. The other models illustrated use the optimized architecture at the given generation number. The KDPI-only is used as ground truth for identifying hard-to-place kidneys. The average is for the full-scale model across the elite population of ten. The KDPI-characteristics model is using ten characteristics that regress KDPI but not KDPI itself.

Table 5 displays recognition accuracy (%) on the deceased-donor dataset prediction for kidney disposition. The best accuracy is the fitness (kidney disposition prediction) of the best deep learning architecture generated by the genetic algorithm and shown in encoded format per chromosome notation shown in Figure 3. The KDPI-char is an abbreviation of the KDPI-characteristic model using the ten KDPI characteristics. The final layer of the deep architecture uses the SoftMax function (normalized exponential function) to normalize kidney disposition prediction over 'transplant' or 'discard' classes. Hence, the kidney disposition results can be presented regarding the likelihood of the kidney being transplanted or discarded. Thus, OPOs could assign a probability threshold value to determine when to engage in accelerated placement.

TABLE 5
GENETIC ALGORITHM DEEP ARCHITECTURE RESULTS FOR KIDNEY DISPOSITION

Genera tion	Best architecture %	KDPI-char %	Best deep architecture using bit-representation
01	87.11	83.10 00	00 000 01 01 0 001 10 11 00 0
02	87.59	83.52 00	00 000 01 01 0 100 10 11 00 0
03	88.11	83.91 00	01 010 01 01 0 100 11 11 01 0
04	89.12	84.23 00	01 010 00 00 0 001 11 11 01 1
05	89.57	84.92 00	01 010 01 01 0 111 11 11 01 1
10	92.81	86.93	01 011 01 01 0 101 11 11 01 1
15	93.12	87.43 00	01 011 01 01 0 101 11 10 01 1
20	93.12	87.92 00	01 011 01 01 0 101 11 10 01 1
30	93.12	88.24 00	01 011 01 01 0 101 11 10 01 1
40	93.12	88.24 00	01 011 01 01 0 101 11 10 01 1

The KDPI-char model provides increased accuracy in representing deceased donor kidneys about their disposition compared to KDPI. This result indicates that KDPI is a critical projection of longevity matching allocation [39] (matching kidneys with the recipient's long-term prognosis) but is a poor predictor of kidney discard [40]. One of the rationales for model prediction variations may be attributed to the high correlation between hypertension and kidney disposition and the correlation between diabetes and kidney disposition. Yet, both are given a lower profile when calculating KDPI. The KDPI calculation regards hypertension and diabetes using binary representation (yes/no), whereas the trained KDPI-char model considers the duration-incremental effect. This model can help support early engagement in accelerated placement using only limited deceased donor characteristics.

Figure 5 presents the confusion matrix of the best deep learning architecture, followed by the classification report showing each class's precision, recall, and f1-score. Class 1 represents a transplanted kidney, whereas class 0 implies a discard for the kidney disposition classification. As noted from the confusion matrix, the quadrant representing missed opportunities is the

false positives (FPs), where historically, the kidney is discarded, but the prediction is to transplant the kidney. The kidneys in the FP quadrant have a mean KDPI of 74. The majority are expanded-criteria donors with a mean clamp time (time of procurement) of 13:40, and 95% are connected to the pump (machine perfusion to improve the preservation of kidneys during storage).

n = 6330	Actual: 1	Actual: 0	
Predicted: 1	5149	376	5525
Predicted: 0	59	746	805
V	5208	1122	

Class 1 (transplant) Class 0 (discard)
Accuracy Score: 0.9312796209
Classification Report:
 precision recall f1-score support
1 0.93 0.99 0.96 5208

0.77

1141

Figure 5. The confusion matrix and classification report are shown for the hard-to-place full-scale after-procurement kidney model. At a threshold value of .5, the model is optimistically inferring that 376 of the discarded kidneys should have been transplanted. Similarly, the model is predicting 59 of the transplanted kidneys should have been discarded.

0.66

0

0.93

Figure 6 illustrates the historical kidney discard rate for recovered and not transplanted kidneys and four predictive models using the deep architecture illustrated earlier. The 'Data Discard' line presents the discard rate of kidneys using the OPTN data range mentioned earlier in our research. The KDPI and KDPI-serum prediction models are used as baseline models. In addition, we created two other models to aid early engagement in accelerated placement decision-making. All models surpass the KDPI-only model suggesting that KDPI alone should not be a kidney disposition predictor. This plot is assembled to show the influence of deceased donor characteristics, available before procurement, on predicting kidney disposition and early recognition of kidneys at risk of discard. The KDPI-char model closely matches the full-scale procurement model, denoting that additional characteristic might not significantly contribute to predicting hard-to-place kidneys. This empowers OPOs in quickly identifying hard-to-place kidneys even before the kidneys have been procured.

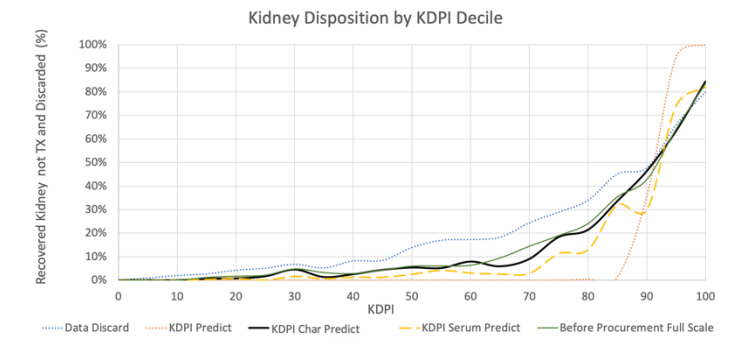


Figure 6. Historical kidney discard and four models predicting discard rate based on KDPI only, KDPI characteristics, KDPI and serum creatinine, and a full-scale model that uses all characteristics shown in Table 2, excluding

procurement biopsy results. This Figure shows models that used deceased donor kidney characteristics before procurement. The best performer following the discard rate closely is the full-scale before-procurement model at 91.4 % accuracy. The next leading model is the ten KDPI characteristics model yielding 89.2 % accuracy, followed by the KDPI-serum model at 84.9 % accuracy. KDPI-only model accuracy is at 83.1 %.

Similarly, Figure 7 illustrates the historical kidney discard rate for recovered and not transplanted kidneys and three predictive models using the same deep learning architecture. Historical kidney discards and full-scale before procurement models are the same as in Figure 6. The added models are the baseline model using KDPI, age, and biopsy results and the full-scale model like the one shown in Figure 6 but added procurement biopsy results to the model input.

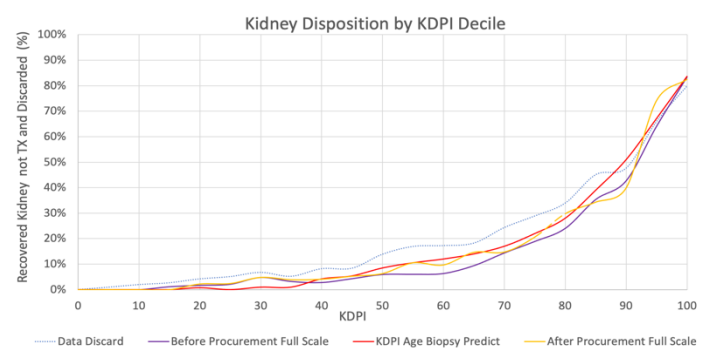


Figure 7. Historical kidney discard and three models predicting discard rate based on KDPI-age-biopsy, full-scale before-procurement model, and full-scale after-procurement model. The best performer that closely follows the discard rate is the full-scale after-procurement model at 93.1 % accuracy, followed by the full-scale before procurement at 91.4 % accuracy. The leading model of all benchmark models is the KDPI-age-biopsy model at 89.8% accuracy. Although historical kidney discard is greater than the leading benchmark model, there might be an unnecessary discard in the lower-KDPI deciles by using the leading benchmark model (KDPI-age-biopsy).

The KDPI-age-biopsy model is the front-runner of the baseline models that OPOs may internally practice for accelerating kidney placements. However, even with biopsy results, this model does not convey much value-added deceased donor information that cannot be acquired from clinical deceased donor information [41] readily available before procurement with no added exacerbations of accrued CIT. From Figure 7, we note that biopsy increases discard for low KDPI kidneys beginning with KDPI 35 to 85 range with a significant increase in discard for KDPI 50 to 70 range. Although now it is mandatory to perform a biopsy for expanded criteria donors, donors with KDPI greater than 85, donors with a history of diabetes and hemoglobin of 6.5 or greater, etc., biopsy for lower KDPI may lead to unnecessary discard. On the other hand, the clamp time, although correlated with kidney disposition, did not significantly affect the model prediction. We suggest that it may have a greater influence when linked with the day of the week since deceased donor kidneys are harder to place on the weekends [10] and can be used as a surrogate for early engagement in the accelerated placement. All models shown in Figure 7 are more optimistic and suggest that there may have been an increase in kidney transplantation for high-risk kidneys with early engagement in accelerated placement.

4 DISCUSSIONS

The research focuses on leveraging AI opportunities to aid in identifying kidneys that are hard to place for early engagement in accelerated placement. This approach uses historical OPTN deceased donor data to model kidney disposition. Convolutional neural networks tuned by a genetic algorithm develop the deep learning architecture that enhances prediction accuracy compared to three baseline ground truth models. Compared to the most common baseline of KDPI as the sole predictor for kidney discard, our full-scale after procurement model shows a ten percent increase in correctly predicting donor disposition. These trained kidney disposition models that can be used anytime during the kidney allocation process will aid OPOs in assessing if the deceased donor kidney is hard to place using currently available deceased donor clinical characteristics. The models allow OPOs to deviate from the match-run and avoid the exacerbations caused by cold ischemic time.

Because most deceased donor kidney discards happen for KDPI 80 or higher, KDPI is used as a surrogate for predicting discard. This research found that KDPI alone should not be used as a predictor to identify hard-to-place kidneys at risk of discard, instead, added clinical characteristics will significantly improve the prediction of deceased donor kidney disposition. Also, the study recovered that biopsy may not yield much-added information about the deceased donor that cannot be acquired from clinical characteristics. Yet it may cause unnecessary discard of lower KDPI deceased donor kidneys.

Despite the excellent results, our proposed approach may have some limitations. The results are not unique and may vary on the nature of the data, data input features, data imputations and preprocessing, architecture style limitations, or limitations of the framework (tools and options) used to deploy the genetic algorithm. In addition, deceased donor characteristics are only one component of a complex kidney allocation system; many other factors must be considered. Perhaps the best way to assess the proposed approach is to have subject experts test the hard-to-place kidney models and observe their effect on reducing deceased donor kidney discards.

The need for a more structured approach lays the foundation for future work to develop a novel many-objective optimization. The many-objective approach creates data-adaptive deep learning architectures using OPO and transplant centers' objectives.

Funding Sources: None

Disclosure: The authors of this manuscript have no conflicts of interest to disclose

Data availability statement: The data reported here have been supplied by the United Network for Organ Sharing as the contractor for the Organ Procurement and Transplantation Network. The interpretation and reporting of these data are the responsibility of the Author (s) and in no way should be seen as an official policy or interpretation by the OPTN or the U S Government. The data that support the findings of this study are openly available in SRTR 2206 Public SAFs Data Dictionary at https://optn.transplant.hrsa.gov/data/

REFERENCES

- [1] Axelrod DA, Schnitzler MA, Xiao H, et al. An economic assessment of contemporary kidney transplant practice. *American Journal of Transplantation*. 2018;18(5):1168-1176. doi:10.1111/ajt.14702
- [2] Wolfe RA, Ashby VB, Milford EL, et al. Comparison of mortality in all patients on dialysis, patients on dialysis awaiting transplantation, and recipients of a First cadaveric transplant. New England Journal of Medicine. 1999;341(23):1725-1730. doi:10.1056/nejm199912023412303
- [3] Hart A, Lentine KL, Smith JM, et al. OPTN/SRTR 2019 Annual data report: Preface. American Journal of Transplantation. 2021;21(S2):1-10. doi:10.1111/ajt.16497
- [4] How organs are matched. Transplant Living https://transplantliving.org/before-the-transplant/about-organ-allocation. Published March 24, 2022. Accessed September 10, 2022.
- [5] King KL, Chaudhry SG, Ratner LE, Cohen DJ, Husain SA, Mohan S. Declined offers for deceased donor kidneys are not independent of organ quality. *Kidney360*. 2021;2(11):1807-1818. doi:10.34067/kid.0004052021
- [6] Kidney Accelerated Placement Project launched in 2019. UNOS. https://unos.org/news/kidney-accelerated-placement-project-for-national-offers-begins-july-18/. Published February 20, 2020. Accessed September 15, 2022.
- [7] King KL, Husain SA, Perotte A, Adler JT, Schold JD, Mohan S. Deceased donor kidneys allocated out of sequence by Organ Procurement Organizations. *American Journal of Transplantation*. 2022;22(5):1372-1381. doi:10.1111/ajt.16951
- [8] Klarman SE, Formica RN. The broader sharing of deceased donor kidneys is an ethical and legal imperative. *Journal of the American Society of Nephrology*. 2020;31(6):1174-1176. doi:10.1681/asn.2020020121
- [9] For Transplant Center Professionals. https://www.srtr.org/faqs/for-transplant-center-professionals/#h2porgans. Accessed September 14, 2022.
- [10] King KL, Husain SA, Cohen DJ, Mohan S. Deceased donor kidneys are harder to place on the weekend. *Clinical Journal of the American Society of Nephrology*. 2019;14(6):904-906. doi:10.2215/cjn.00620119
- [11] Konieczny A, Stojanowski J, Rydzyńska K, Kusztal M, Krajewska M. Artificial Intelligence—a tool for risk assessment of delayed-graft function in kidney transplant. *Journal of Clinical Medicine*. 2021;10(22):5244. doi:10.3390/jcm10225244
- [12] Luo Y, Liang J, Hu X, et al. Deep learning algorithms for the prediction of posttransplant renal function in deceased-donor kidney recipients: A preliminary study based on pretransplant biopsy. *Frontiers in Medicine*. 2022;8. doi:10.3389/fmed.2021.676461
- [13] Rashidi P, Bihorac A. Artificial intelligence approaches to improve kidney care. *Nature Reviews Nephrology*. 2019;16(2):71-72. doi:10.1038/s41581-019-0243-3
- [14] Berrar D, Dubitzky W. Deep Learning in Bioinformatics and biomedicine. *Briefings in Bioinformatics*. 2021;22(2):1513-1514. doi:10.1093/bib/bbab087
- [15] Tan JH, Hagiwara Y, Pang W, et al. application of stacked convolutional and long short-term memory network for accurate identification of CAD ECG signals. *Computers in Biology and Medicine*. 2018;94:19-26. doi:10.1016/j.compbiomed.2017.12.023
- [16] Acharya UR, Fujita H, Oh SL, Hagiwara Y, Tan JH, Adam M. Application of deep convolutional neural network for automated detection of myocardial infarction using ECG signals. *Information Sciences*. 2017;415-416:190-198. doi:10.1016/j.ins.2017.06.027
- [17] Ferrarese A, Sartori G, Orrù G, et al. Machine learning in liver transplantation: A tool for some unsolved questions? *Transplant International*. 2021;34(3):398-411. doi:10.1111/tri.13818
- [18] Threlkeld R, Ashiku L, Canfield C, et al. Reducing kidney discard with artificial intelligence decision support: The need for a transdisciplinary systems approach. *Current Transplantation Reports*. 2021;8(4):263-271. doi:10.1007/s40472-021-00351-0
- [19] Ashiku L, Threlkeld R, Canfield C, Dagli C. Identifying AI opportunities in donor kidney acceptance: Incremental hierarchical systems engineering approach. 2022 IEEE International Systems Conference (SysCon). 2022. doi:10.1109/syscon53536.2022.9773875
- [20] Gottapu RD, Dagli CH. Efficient architecture search for Deep Neural Networks. *Procedia Computer Science*. 2020;168:19-25. doi:10.1016/j.procs.2020.02.246
- [21] Ashiku L, Dagli C. Network intrusion detection system using deep learning. *Procedia Computer Science*. 2021;185:239-247. doi:10.1016/j.procs.2021.05.025
- [22] Nandini B. Detection of skin cancer using Inception V3 and Inception V4 Convolutional Neural Network (CNN) for Accuracy Improvement. Revista

- *Gestão Inovação e Tecnologias*. 2021;11(4):1138-1148. doi:10.47059/revistageintec.v11i4.2174
- [23] Zhang C, Benz P, Argaw DM, et al. Resnet or DenseNet? introducing dense shortcuts to resnet. 2021 IEEE Winter Conference on Applications of Computer Vision (WACV). 2021. doi:10.1109/wacv48630.2021.00359
- [24] Loni M, Sinaei S, Zoljodi A, Daneshtalab M, Sjödin M. DeepMaker: A multi-objective optimization framework for deep neural networks in embedded systems. *Microprocessors and Microsystems*. 2020;73:102989. doi:10.1016/j.micpro.2020.102989
- [25] Ostraich B, Kochavi E, Nizri E, Cohen I. Why do shallow caps deflect more than Deep ones? *Journal of Pressure Vessel Technology*. 2005;128(3):476-478. doi:10.1115/1.2218354
- [26] Drozdzal M, Vorontsov E, Chartrand G, Kadoury S, Pal C. The importance of skip connections in biomedical image segmentation. *Deep Learning and Data Labeling for Medical Applications*. 2016:179-187. doi:10.1007/978-3-319-46976-8
- [27] Balagourouchetty L, Pragatheeswaran JK, Pottakkat B, Ramkumar G. GoogLeNet-based ensemble FCNet classifier for focal liver lesion diagnosis. *IEEE Journal of Biomedical and Health Informatics*. 2020;24(6):1686-1694. doi:10.1109/jbhi.2019.2942774
- [28] Ashiku L, Al-Amin M, Madria S, Dagli C. Machine learning models and big data tools for evaluating kidney acceptance. *Procedia Computer Science*. 2021;185:177-184. doi:10.1016/j.procs.2021.05.019
- [29] Xie L, Yuille A. Genetic CNN. 2017 IEEE International Conference on Computer Vision (ICCV). 2017. doi:10.1109/iccv.2017.154
- [30] Ghaheri, A., Shoar, S., Naderan, M., & Hoseini, S. S. (2015). The applications of genetic algorithms in medicine. *Oman Medical Journal*, 30(6), 406–416. https://doi.org/10.5001/omj.2015.82
- [31] Kim J, Yoo S. Software review: DEAP (distributed evolutionary algorithm in python) library. Genetic Programming and Evolvable Machines. 2018;20(1):139-142. doi:10.1007/s10710-018-9341-4
- [32] De Rainville F-M, Fortin F-A, Gardner M-A, Parizeau M, Gagné C. DEAP. Proceedings of the fourteenth international conference on Genetic and evolutionary computation conference companion - GECCO Companion '12. 2012. doi:10.1145/2330784.2330799
- [33] Kim US, Mahroo OA, Mollon JD, Yu-Wai-Man P. Retinal ganglion cells—diversity of cell types and clinical relevance. Frontiers in Neurology. 2021;12. doi:10.3389/fneur.2021.661938
- [34] Smith JH, Rowland C, Harland B, et al. How neurons exploit fractal geometry to optimize their network connectivity. *Scientific Reports*. 2021;11(1). doi:10.1038/s41598-021-81421-2
- [35] Yu F, Wang D, Shelhamer E, Darrell T. Deep layer aggregation. 2018 IEEE/CVF Conference on Computer Vision and Pattern Recognition. 2018. doi:10.1109/cvpr.2018.00255
- [36] Lentine KL, Naik AS, Schnitzler MA, et al. Variation in use of procurement biopsies and its implications for discard of deceased donor kidneys recovered for transplantation. *American Journal of Transplantation*. 2019;19(8):2241-2251. doi:10.1111/ajt.15325
- [37] Zhou S, Massie AB, Holscher CM, et al. Prospective validation of prediction model for kidney discard. *Transplantation*. 2019;103(4):764-771. doi:10.1097/tp.00000000000002362
- [38] Marrero WJ, Naik AS, Friedewald JJ, et al. Predictors of deceased donor kidney discard in the United States. *Transplantation*. 2017;101(7):1690-1697. doi:10.1097/tp.0000000000001238
- [39] Querard A-H, Foucher Y, Combescure C, et al. Comparison of survival outcomes between expanded criteria donor and standard criteria donor kidney transplant recipients: A systematic review and meta-analysis. *Transplant International*. 2016;29(4):403-415. doi:10.1111/tri.12736
- [40] Arias-Cabrales C, Pérez-Sáez MJ, Redondo-Pachón D, et al. Usefulness of the KDPI in Spain: A comparison with donor age and definition of standard/expanded criteria donor. *Nefrología*. 2018;38(5):503-513. doi:10.1016/j.nefro.2018.03.003
- [41] Lentine KL, Fleetwood VA, Caliskan Y, et al. Deceased donor procurement biopsy practices, interpretation, and histology-based decisionmaking: A survey of US kidney transplant centers. *Kidney International Reports*. 2022;7(6):1268-1277. doi:10.1016/j.ekir.2022.03.021